PHOTONICS Research

Carrier localization in InGaN by composition fluctuations: implication to the "green gap"

Sergey Yu Karpov

STR Group—Soft-Impact, Ltd., P.O. Box 83, 27 Engels Ave., St. Petersburg 194156, Russia (sergey.karpov@str-soft.com)

Received 1 November 2016; revised 23 January 2017; accepted 24 January 2017; posted 25 January 2017 (Doc. ID 279871); published 23 February 2017

A simple semi-empirical model for radiative and Auger recombination constants is suggested, accounting for hole localization by composition fluctuations in InGaN alloys. Strengthening of fluctuation with the indium molar fraction in InGaN is found to be largely responsible for decreases in both the radiative and Auger recombination constants with emission wavelength. The model provides good fitting of the experimental spectral dependencies of the recombination constants, thus demonstrating implication of the carrier localization to light-emitting diode efficiency reduction in the "green gap."

OCIS codes: (130.0250) Optoelectronics; (160.6000) Semiconductor materials; (230.3670) Light-emitting diodes; (250.5590) Quantum-well, -wire and -dot devices; (260.3800) Luminescence.

https://doi.org/10.1364/PRJ.5.0000A7

1. INTRODUCTION

Big progress in InGaN light-emitting diode (LED) fabrication technology in the recent decade has resulted in demonstration of the devices with maximum external quantum efficiency (EQE) over ~80% in the violet–blue spectral range [1,2] (see also a summary of the data given in [3]). Such LEDs still suffer from efficiency droop, i.e., substantial non-thermal EQE reduction at high currents, a problem for which a number of effective approaches to solution have already been proposed [4]. However, expansion of the LED emission wavelength to the green and then to the yellow spectral range leads to much lower maximum EQE values, namely ~40% – 50% [5,6] and ~20% [7], respectively. This efficiency decline with the wavelength is known as the "green gap" problem. The efficiency reduction is not related to insufficient light extraction from the LED dice [3]. In addition remarkable increase in the threshold current density and decrease of the wall-plug efficiency of InGaN-based laser diodes is also observed in the same spectral range [8,9]. All this enables attributing the above phenomena to internal processes occurring in the active regions of the LEDs and laser diodes.

There are two commonly accepted explanations for the green gap. One associates the reduction of LED internal quantum efficiency (IQE) with the crystal quality degradation in InGaN quantum wells (QWs) under increasing the indium molar fraction in the alloy [10]. Indeed, higher indium concentration necessary for green/yellow light emission produces a larger lattice constant mismatch between InGaN and underlying GaN, which may initiate stress relaxation in InGaN accompanied by dislocation formation, if the QW width becomes larger than its critical value. Estimations of the (0001) InGaN/GaN critical thickness show that it becomes comparable with the typical QW widths in the green/yellow spectral range [11]. Even if stress relaxation does not occur, the crystal quality of InGaN may, nevertheless, worsen because of lower growth temperatures typically used for increasing the indium incorporation into InGaN QWs, which favors point defect formation and parasitic impurity incorporation [12].

In order to understand, if the crystal quality degradation may be the principal reason for the IQE reduction, it is worth looking at the recombination constants normally derived from the popular *ABC* model, considering carrier recombination in InGaN QWs to occur via three main channels: Shockley–Read–Hall non-radiative recombination at point and extended defects (the respective recombination constant is A), radiative recombination (with the constant B), and Auger non-radiative recombination (with the constant C). These constants can be evaluated in one way or another from the joint measurements of EQE and differential carrier lifetime in the LED active region as a function of operating current [13–15]. The data reported in [15] for industrial-grade LED structures show, in particular, the A-constant not to vary noticeably in the spectral range from 400 to 515 nm, where the green gap is already quite pronounced. This means that the crystal quality degradation with the indium content in InGaN QWs is not the principal reason for the green gap.

The second commonly accepted explanation for the green gap invokes built-in polarization fields resulting in spatial separation of the electron and hole wave functions in (0001)

InGaN QWs [16] and, thus, in lowering of the B-constant with increasing indium molar fraction in the alloy [17]. In addition, substantial increase in the Auger recombination rate has been predicted theoretically for high polarization fields [18], reducing further the LED efficiency. However, no remarkable difference between the green gap behavior in polar and nonpolar/semipolar LED structures, where the polarization field is eliminated/reduced, was observed to date in spite of natural expectations [19]. So, the built-in polarization field in the (0001) structures cannot alone be considered as the principal factor determining the green gap, similarly to the degradation of the InGaN crystal quality.

This paper is aimed at analyzing the impact of carrier localization in InGaN alloys by composition fluctuations on the radiative and Auger recombination. Using a unified semi-empirical model, the implication of carrier localization into the green gap problem will be demonstrated. Earlier, the localization phenomenon was invoked to explain non-exponential carrier dynamics in time-resolved photoluminescence experiments [20], and a rather high IQE of InGaN-based LEDs achieved despite a huge threading dislocation density inherent in III-nitride epitaxial materials grown on sapphire substrates [21]. The latter issue is directly related to localization impact on the non-radiative recombination constant A. This paper will show that other recombination coefficients, B and C, may be affected remarkably by carrier localization, as well.

2. MODEL

A. Recombination Constants

To study the localization effect on the recombination processes, a simple semi-empirical model is suggested, regarding electrons as the carriers delocalized in the conduction band and holes as those strongly localized by composition fluctuations in a bulk InGaN alloy. The assumed difference in the localization degree of electrons and holes is attributed to the hole effective mass, which is much heavier than that of electrons. The localization strength will be characterized by the localization energy E_L. Assuming for simplicity the wave functions of localized holes to be like that in the hydrogen atom, one can determine the radius of localization: $a_L = \hbar/(2m_h E_L)^{1/2}$, where $\hbar$ is Planck's constant, and m_h is the heavy-hole effective mass. The optical transition between a delocalized electron represented by a plane wave and a localized hole can be considered similarly to impurity-mediated radiative recombination [22], providing for the radiative recombination constant the approximate expression

$$B = 64\pi\nu_B a_L^3 \xi^4; \qquad \nu_B = \frac{2\alpha n_r E_g E_P}{3\hbar m_0 c^2}, \qquad \xi = \frac{m_h E_L}{m_h E_L + m_e E_e}. \tag{1}$$

Here, ν_B is the specific frequency of optical transitions, α is the fine-structure constant, n_r is the group refractive index of the semiconductor, E_g is its energy gap, $E_P = 2m_0 P^2$ is the energy associated with the Kane's matrix element P, m_0 is the electron mass, c is the light velocity, and m_e is the effective mass of electrons. The parameter E_e is the mean kinetic energy of electrons, which equals kT (k is the Boltzmann constant and T is temperature) in the case of non-degenerate electrons and is nearly equal to $\frac{1}{2}F_n$ (F_n is the quasi-Fermi level position counted from the conduction band edge), if electrons are degenerate. It is important that the optical transitions do not require any momentum selection rule because of hole localization, which enhances the transition rate.

In a similar manner, the Auger recombination process involving two delocalized electrons and a localized hole can be considered. The process implies energy transfer from one electron to another due to their Coulomb collision. If the energy transferred from the first electron to the second one becomes comparable with E_g, the first electron can recombine with the localized hole. At that, the rate of the electron energy loss is regarded as the limiting stage of the whole Auger process. To calculate the rate of such Auger recombination, the approach suggested in [23] for impurity-assisted Auger processes can be applied. As a result, the Auger recombination constant C can be estimated from the expression

$$C = \frac{64\pi^2}{3}\frac{E_B}{\hbar}\left(\frac{E_e}{E_g}\right)a_L^3 a_G^3 \ln\Lambda; \qquad a_G = \frac{\hbar}{[2m_e(E_g - E_L)]^{1/2}}. \tag{2}$$

In Eq. (2), $E_B/\hbar$ is the frequency typical for the Auger processes involving two electrons and a hole, E_B is the binding energy of a shallow donor in InGaN, and $\ln\Lambda$ is the so-called Coulomb logarithm. The authors of [23] neglected the numerical factors and Coulomb logarithm in expressions similar to Eq. (2), regarding their results as those obtained with "logarithmic accuracy." According to [24,25], $\ln\Lambda$ is ~4–7 at electron concentration of $\sim 10^{18}$–10^{19} cm^{-3}. Therefore, the mean value $\ln\Lambda \approx 5.5$ has been chosen for further calculations. The numerical factor in Eq. (2) refines those reported earlier in [3,26].

Equations (1) and (2) show the impact of the hole localization on the recombination constants to be largely accounted for via the localization radius a_L. It is interesting that the C/B ratio does not contain a_L at all. Therefore, this ratio varies slowly with the emission wavelength (InGaN composition), mainly following the variation of the alloy materials parameters. This fact may be used for validation of the suggested model.

Generally, InGaN composition fluctuations produce localized states with various localization energies. Therefore, the parameters a_L or E_L should be regarded as those averaged over the ensemble of localized holes [26].

B. Localization Energy

One of the approaches suggested for estimating the localization energy in conventional III–V alloys was the phenomenological optimal-fluctuation method (see, e.g., review [27] and references therein). The theory provides the following estimate for the localization energy:

$$E_L = \frac{\alpha_h^4 x^2 (1-x)^2 m_h^3}{\gamma\hbar^6 N^2}, \qquad \gamma = 18\pi^2 \approx 178. \tag{3}$$

Here, x is the molar fraction of InN in InGaN alloy, $\alpha_h = dE_v/dx$ is the rate of the valence band edge E_v variation with x, and N is the density of the cation sites in the InGaN crystal lattice.

Estimation of E_L made by Eq. (3) assuming $dE_v/dx \approx \frac{1}{2}dE_g/dx$ provides localization energy of ~12–18 meV in the blue–green spectral range. Unfortunately, the optimal-fluctuation method is not applicable directly to InGaN alloys. First, this approach has been developed for ideal ternary compounds having negligible mixing enthalpy. So, the strong non-ideality of InGaN alloys, as well as the strain impact on the optimal fluctuation, is not accounted for in Eq. (3). Second, detailed analysis shows that the optimal fluctuation contains ~6–8 atoms of indium only. This violates the basic assumptions underlying the phenomenological optimal-fluctuation model, invoking atomistic approaches as those more suitable for simulation of hole localization.

The atomistic nature of hole localization was demonstrated for the first time in [28] for zinc-blende InGaN alloys, using *ab initio* calculations based on density-functional theory (DFT). Later, similar results were obtained for wurtzite InGaN QWs by tight-binding (TB) calculations [29,30]. Whereas electron delocalization in the conduction band was established by DFT [26], the TB simulations predicted both electrons and holes to be localized by composition fluctuations [29,30] but in regions with essentially different dimensions. At that, both the vertical separation of electron and hole wave functions due to the polarization field and their localization at different lateral positions inside the QWs led to reducing oscillation strengths of optical transitions.

Unfortunately, the *ab initio* simulations could not provide the guiding information on the ensemble-averaged hole localization radius or localization energy. Therefore, for the purpose of comparison of the present approach with available data and results of other theories, the general dependence $E_L(x)$ coming from Eq. (3) has been accepted: $E_L(x) = E_t x^2(1-x)^2$, with E_t being a fitting parameter.

3. RESULTS

A. Localization Radius and Energy Factor

Figure 1(a) shows the hole localization radius a_L and energy factor ξ as a function of emission wavelength calculated at $E_t = 1.85$ eV for different electron energies varied from 26 meV (kT at room temperature) to 80 meV. The value of E_t was chosen to provide the best fitting of the relative variation of B- and C-constants with the wavelength, regardless of their absolute values. This corresponds to localization energy variation from ~35 to ~85 meV in the spectral range of 450–540 nm covered by the measurements of recombination constants reported in [15]. Dependence of the electron and hole effective masses on the InGaN composition was taken into account by the known scaling of m_e with E_g and E_P [31] and linear interpolation of the hole effective masses calculated in [32].

In contrast to the energy factor, which tends to saturate at longer wavelengths, the radius a_L changes considerably with the wavelength, providing the major contribution to variation of the recombination constant, according to Eqs. (1) and (2).

Experimental and calculated B/C ratios are plotted in Fig. 1(b) versus emission wavelength. It is seen from their comparison that the electron energy of 40 meV provides the best fitting of the data reported in [15].

B. Radiative Recombination Constant

Figure 2(a) compares the experimental spectral dependence of the B-constants [15] with the values calculated using conventional approaches. Those corresponding to bulk InGaN (B_{3D}) and QWs (B_{QW}) have been determined by the expressions

$$B_{3D} = \nu_B/N_{CV}, \qquad B_{\mathrm{QW}} = \nu_B\Omega/N_{\mathrm{QW}}d_{\mathrm{QW}},$$
$$N_{CV} = 2[(m_e + m_h)kT/2\pi\hbar^2]^{3/2},$$
$$N_{QW} = 2[(m_e + m_h)kT/2\pi\hbar^2]. \tag{4}$$

Here, N_{CV} and N_{QW} are the joint effective densities of states of the bulk alloy and QW, respectively, d_{QW} is the QW width, and Ω is the square of the overlap integral of the ground-state electron and hole wave functions in the QW. The overlap integral has been evaluated numerically for the case of a single quantum well (SQW) LED structure with variable InGaN composition in the QW, using the commercial SiLENSe 5.11 package [33].

One can see from Fig. 1(a) that B_{3D} depends rather weakly on the emission wavelength, whereas B_{QW} declines more steeply because of decreasing overlap between the electron and hole wave functions originated from the built-in polarization field. However, the slope of the curves is still insufficient to fit the experimental variation of the B-constant.

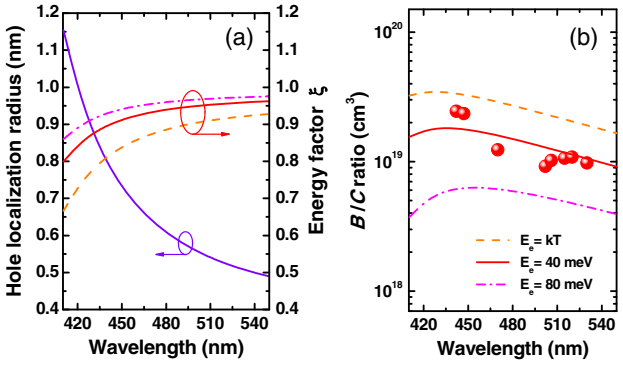

Fig. 1. (a) Hole localization radius and energy factors corresponding to different electron kinetic energies E_e and (b) B/C ratio as a function of emission wavelength. Balls are data from [15], lines are calculations.

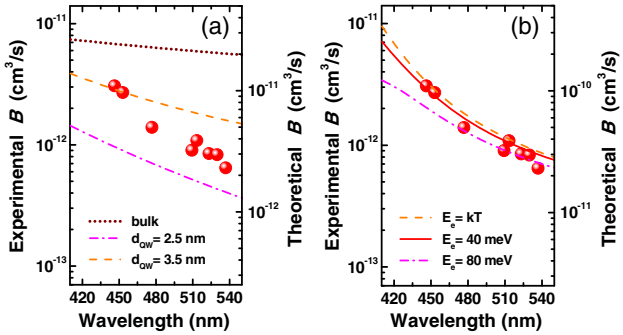

Fig. 2. Experimental [15] (balls) and theoretical (lines) radiative recombination constants calculated for (a) bulk InGaN and representative QWs and (b) for bulk InGaN with account of hole localization at different electron kinetic energies. Note that theoretical scales are shifted with respect to experimental one for better comparison of spectral dependence of the B-constants.

In contrast, calculation of the B-constant by Eq. (1) provides a good fitting of its experimental dependence on the emission wavelength, weakly changing with the electron kinetic energy E_e [Fig. 2(b)]. The steep decrease of the B-constant with the wavelength originates here from the respective decrease in the radius a_L due to a stronger hole localization by composition fluctuations at longer wavelengths, which is directly related to reducing the overlap of the localized hole/delocalized electron wave functions.

C. Auger Recombination Constant

Auger recombination in III-nitride LEDs is commonly explained in terms of indirect phonon-assisted processes occurring in the bulk InGaN alloys [34,35]. This is because simulations of [34,35] provide a close quantitative correlation with the absolute values of the C-constants reported in [15]. However, the slopes of the theoretical curves are opposite of the observed ones [see Fig. 3(a)]. Also, both models [34,35] predict the Auger process involving two holes and one electron to be nearly twice as intensive as the process involving two electrons and a hole. The latter prediction is not in line with the recent data of [36] likely supporting the opposite trend.

Direct Auger recombination in InGaN QWs has been considered in [18,37]. A resonant dependence of the Auger recombination constant on the well width was predicted in [37] for an $In_{0.25}Ga_{0.75}N$/GaN QW: the C-constant reached its maximum value of $\sim 5 \times 10^{-31}$ cm^6/s at $d_{QW} = 2$ nm and practically vanished at $d_{QW} = 3$ nm. Strong increase in the Auger recombination rate and simultaneous decrease in the radiative recombination rate with the magnitude of the polarization field in a QW was obtained in [18], which implies remarkable improvement of the LED efficiency in the green gap and suppression of its droop with current in nonpolar/semipolar LEDs. Unfortunately, neither of the predicted trends correlated with available observations, indicating involvement of additional obscured mechanisms. Accounting for the hole localization in InGaN, using Eq. (2), provides, in contrast, good fitting of the experimental wavelength dependence of the C-constant [Fig. 3(b)], similar to the radiative recombination constant. Here, the electron kinetic energy is found to affect noticeably the absolute value of the C-constant, determining its dependence on the carrier concentration. By its nature, the considered Auger process involves two electrons and a localized hole, which agrees with the conclusions made in [36].

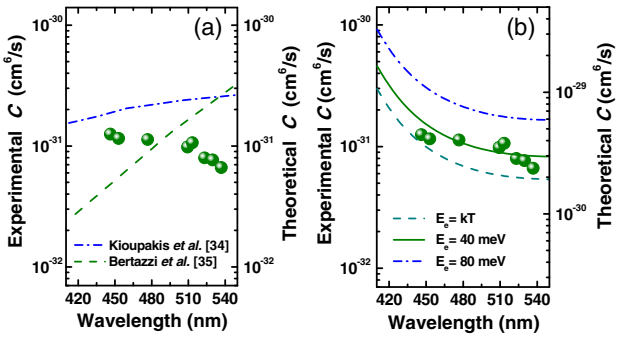

Fig. 3. Experimental [15] (balls) and theoretical (lines) total Auger recombination constants calculated for (a) bulk InGaN with the account of phonon-assisted processes and (b) hole localization. Note that theoretical scales are shifted with respect to the experimental one for better comparison of spectral dependence of the C-constants.

D. Discussion

Though the model accounting for hole localization fits pretty well the experimental spectral dependence of the radiative and Auger recombination constants [Figs. 2(b) and 3(b)], the predicted absolute values of the constants are overestimated by a factor of ~35 (note different vertical scales for experimental and theoretical values in the figures). The calculated B-constant is even greater than that estimated for bulk InGaN without accounting for localization. This fact is attributed to breaking the momentum selection rule in the case of localized holes. The main reason for the discrepancy between the data of [15] and predictions of the semi-empirical model is neglecting the spatial separation of the electron and hole wave functions caused by the polarization field in (0001)InGaN/GaN QWs. So, the above model seems to be more applicable to nonpolar/semipolar LED structures with vanished/reduced polarization fields than to polar ones. In the latter case, the results of the semi-empirical model should be considered as qualitative ones only.

From this point of view, it is worth comparing the results obtained for the B-constant by the semi-empirical model and by atomistic simulations reported in [30] for polar InGaN QWs. Accounting for a dozen of the lowest electron and hole states and being scaled by a factor of ~1.5–3.0, the simulations reproduce quite well the experimental wavelength dependence of the B-constant (see supplemental materials to [30]). Using, then, the data on the recombination constants A and C borrowed from [15], the authors of [30] have identified the percentage of the IQE reduction in the green gap related to the polarization field (~70%) and carrier localization (~30%). Based on these predictions, remarkable IQE improvement is expected in nonpolar/semipolar LEDs with similar active region designs, which is not confirmed experimentally [19,38]. On the other hand, 100% contribution of hole localization to the IQE reduction assumed by the present semi-empirical model seems to be also overestimated. Therefore, determination of the actual percentage for the contributions is one of the most important tasks for future studies, as it may open new ways for the LED efficiency improvement in the green gap. For this purpose, experimental evaluation of the recombination constants for nonpolar/semipolar LED structures would be very helpful.

Despite the still open question, both the atomistic [30] and the present semi-empirical model demonstrate direct implication of the additional in-plane carrier localization into LED efficiency reduction in the green gap. Indeed, the increase in the localization strength with the indium content in InGaN, or the same, with the emission wavelength results in decreasing overlap between the electron and hole wave functions. This overlap has a 3D character in contrast to the 1D one normally considered as that occurring in polar InGaN QW because of the polarization field. Second, the TB simulations [29,30] predict electrons to be localized by composition fluctuations, too. Uncorrelated electron and hole localization at different lateral positions inside a polar InGaN QW may produce additional reduction of the wave function overlap. The second mechanism is specific for the polar QWs only, where electrons and holes tend to localize next to the opposite interfaces and, hence, in

the regions with different indium atomic configurations. In the absence of a polarization field in the QW, localization of electrons and holes is expected to be correlated, to occur in the same indium-enriched regions, and, thus, to increase the overlap of the electron and hole wave functions. As a nearly similar efficiency decline is observed in the polar and nonpolar/semipolar LED structures (see, e.g., [19,38]), the second mechanism seems to be of secondary importance for the green gap.

For Auger recombination, the semi-empirical model predicts dominance of the process with two electrons and a hole, which correlates with the data of [36]. Indeed, the alternative process involving two localized holes and one electron is expected to be ineffective due to hole localization at different sites, preventing three-particle collisions. Localization of two holes at the same site, which would dramatically enhance Auger recombination, seems to be unlikely because of Coulomb repulsion of the holes. One more alternative mechanism, involving a localized hole, a free hole in the valence band, and a delocalized electron may become important near transition from the localization-mediated to free carrier-mediated recombination. This case requires special examination in the future.

As one can see from Fig. 1(a), the hole localization radius is normally less than typical widths of InGaN QWs, which makes the hole wave function practically independent of the confining potential formed in a particular QW (a similar result has been obtained in [28] for quantum dots by DFT simulations). This fact may explain the absence of the resonant dependence of the C-constant on the QW width predicted earlier in [37].

A critical point of the semi-empirical model is evaluation of the hole localization energy. In this study, E_L was obtained from an appropriate fitting to the data of [15]. In the future, finding reliable ways for experimental evaluation of the localization energy or its correlations with easily measurable parameters seems to be one more important task. It is interesting, in particular, that the values $E_L = 35$–85 meV obtained by fitting in the spectral range of 450–540 nm are found to be just 4 times lower than the corresponding Stokes shifts of the luminescence peaks relative to the optical-absorption edges summarized in [39] for both bulk InGaN layers and QWs.

As it was mentioned above, the localization radius and some other model parameters should generally account for the ensemble properties of localized holes. Using some assumptions on the density of states of localized holes in the energy gap, the model was found to be capable of explaining the anomalous (ascending) temperature dependence of the B-constants reported in [26] for blue and green InGaN QWs. Such a dependence could not be attributed to free carriers either in bulk materials or in QWs.

Finally, the impact of hole localization on the radiative and Auger recombination is expected to be especially valuable in LEDs at low and medium current densities. At high current densities, transition from the localization-mediated recombination to that of delocalized carriers should occur. It would be tempting to get experimental evidence for such a transition and to study it in detail in the future.

4. CONCLUSION

In this paper, a unified semi-empirical model for radiative and Auger recombination constants in bulk InGaN is suggested, accounting for hole localization by composition fluctuations in the alloy and providing good fit for experimental dependence of the constant on the emission wavelength reported in [15]. Along with atomistic simulations [30], the model demonstrates the carrier localization to be an important factor controlling the LED efficiency reduction in the green gap. As it has been shown earlier [26], the semi-empirical model is also capable of explaining the anomalous temperature dependence of the radiative recombination constant observed in both blue and green LED structures.

The basic mechanism underlying the implication of the hole localization to the efficiency green gap is the increase in the localization energy with the indium molar fraction in InGaN, or the same, with the emission wavelength, resulting in considerable reduction of three-dimensional overlap of the electron and hole wave functions. Being suggested for bulk materials, the model seems to also be applicable to nonpolar/semipolar QWs with vanished/reduced built-in polarization fields. For polar QWs, the model requires further elaboration aimed at better understanding of the interplay between the localization-based and polarization-field-based mechanisms of the recombination constant reduction.

From the practical point of view, finding ways for suppression of the composition fluctuation strength in InGaN alloys/QWs by properly adjusting the growth conditions of the LED structures seems to be quite important for closing the green gap. However, statistical fluctuations specific for any randomly disordered alloy may form here a fundamental limitation for the efficiency of long-wavelength III-nitride LEDs.

Funding. European Union Seventh Framework Programme (FP7) (318388).

REFERENCES

1. Y. Narukawa, M. Ichikawa, D. Sanga, M. Sano, and T. Mukai, "White light emitting diodes with super-high luminous efficacy," J. Phys. D **43**, 354002 (2010).
2. C. A. Hurni, A. David, M. J. Cich, R. I. Aldaz, B. Ellis, K. Huang, A. Tyagi, R. A. DeLille, M. D. Craven, F. M. Steranka, and M. R. Krames, "Bulk GaN flip-chip light-emitting diodes with optimized efficiency for high-power operation," Appl. Phys. Lett. **106**, 031101 (2015).
3. S. Y. Karpov, "Light-emitting diodes for solid-state lighting: searching room for improvements," Proc. SPIE **9768**, 97680C (2016).
4. C. Weisbuch, M. Piccardo, L. Martinelli, J. Iveland, J. Peretti, and J. S. Speck, "The efficiency challenge of nitride light-emitting diodes for lighting," Phys. Status Solidi A **212**, 899–913 (2015).
5. M. Peter, A. Laubsch, W. Bergbauer, T. Meyer, M. Sabathil, J. Baur, and B. Hahn, "New developments in green LEDs," Phys. Status Solidi A **206**, 1125–1129 (2009).
6. A. I. Alhassan, R. M. Farrel, B. Saifaddin, A. Mughal, F. Wu, S. P. DenBaars, S. Nakamura, and J. S. Speck, "High luminous efficacy green light-emitting diodes with AlGaN cap layer," Opt. Express **24**, 17868–17873 (2016).
7. S. Saito, R. Hashimoto, J. Hwang, and S. Nunoue, "InGaN light-emitting diodes on *c*-face sapphire substrates in green gap spectral range," Appl. Phys. Express **6**, 111004 (2013).
8. D. Sizov and R. Bhat, "Gallium indium nitride-based green lasers," J. Lightwave Technol. **30**, 679–699 (2012).
9. S. Takagi, M. Ueno, K. Katayama, T. Ikegami, T. Nakamura, and K. Yanashima, "High-power and high-efficiency true green laser diodes," SEI Tech. Rev. **77**, 102–106 (2013).

10. T. Langer, H. Jönen, A. Kruse, H. Bremers, U. Rossow, and A. Hangleiter, "Strain-induced defects as nonradiative recombination centers in green-emitting GaInN/GaN quantum well structures," Appl. Phys. Lett. **103**, 022108 (2013).
11. A. V. Lobanova, A. L. Kolesnikova, A. E. Romanov, S. Y. Karpov, M. E. Rudinsky, and E. V. Yakovlev, "Mechanism of stress relaxation in (0001)InGaN/GaN via formation of V-shaped dislocation half-loops," Appl. Phys. Lett. **103**, 152106 (2013).
12. S. Hammersley, M. J. Kappers, F. C.-P. Massabuau, S.-L. Sahonta, P. Dawson, R. A. Oliver, and C. J. Humphreys, "Effects of quantum well growth temperature on the recombination efficiency of InGaN/GaN multiple quantum wells that emit in the green and blue spectral regions," Appl. Phys. Lett. **107**, 132106 (2015).
13. P. G. Eliseev, M. Osin'ski, H. Li, and I. V. Akimova, "Recombination balance in green-light-emitting GaN/InGaN/AlGaN quantum wells," Appl. Phys. Lett. **75**, 3838–3840 (1999).
14. A. David and M. J. Grundmann, "Droop in InGaN light-emitting diodes: a differential carrier lifetime analysis," Appl. Phys. Lett. **96**, 103504 (2010).
15. D. Schiavon, M. Binder, M. Peter, B. Galler, P. Drechsel, and F. Scholz, "Wavelength-dependent determination of the recombination rate coefficients in single-quantum-well GaInN/GaN light emitting diodes," Phys. Status Solidi B **250**, 283–290 (2013).
16. M. H. Crawford, "LEDs for solid-state lighting: performance challenges and recent advances," IEEE J. Sel. Topics Quantum Electron. **15**, 1028–1040 (2009).
17. K. A. Bulashevich, O. V. Khokhlev, I. Y. Evstratov, and S. Y. Karpov, "Simulation of light-emitting diodes for new physics understanding and device design," Proc. SPIE **8218**, 827819 (2012).
18. R. Vaxenburg, A. Rodina, E. Lifshitz, and A. L. Efros, "The role of polarization fields in Auger-induced efficiency droop in nitride-based light-emitting diodes," Appl. Phys. Lett. **103**, 221111 (2013).
19. M. Pristovsek, C. J. Humphreys, S. Bauer, M. Knab, K. Thonke, G. Kozlowski, D. O'Mahony, P. Maaskant, and B. Corbett, "Comparative study of (0001) and $(11\bar{2}2)$ InGaN based light emitting diodes," Jpn. J. Appl. Phys. **55**, 05FJ10 (2016).
20. A. Morel, P. Lefebvre, S. Kalliakos, T. Taliercio, T. Bretagnon, and B. Gil, "Donor-acceptor-like behavior of electron-hole pair recombinations in low-dimensional (Ga, In)N/GaN systems," Phys. Rev. B **68**, 045331 (2003).
21. S. F. Chichibu, H. Marchand, M. S. Minsky, S. Keller, P. T. Fini, J. P. Ibbetson, S. B. Fleischer, J. S. Speck, J. E. Bowers, E. Hu, U. K. Mishra, S. P. DenBaars, T. Deguchi, T. Sota, and S. Nakamura, "Emission mechanisms of bulk GaN and InGaN quantum wells prepared by lateral epitaxial overgrowth," Appl. Phys. Lett. **74**, 1460–1462 (1999).
22. A. P. Levanyuk and V. V. Osipov, "Edge luminescence of direct-bandgap semiconductors," Sov. Phys. Usp. **24**, 187–215 (1981).
23. V. N. Abakumov, V. I. Perel, and I. N. Yassievich, *Nonradiative Recombination in Semiconductors* (North Holland, 1991).
24. R. Parker, "22.611J Introduction to plasma physics I," MIT OpenCourseWare, 2006, https://ocw.mit.edu.
25. S. A. Khrapak, "Effective Coulomb logarithm for one component plasma," Phys. Plasma **20**, 054501 (2013).
26. F. Nippert, S. Y. Karpov, G. Callsen, B. Galler, T. Kure, C. Nenstiel, M. R. Wagner, M. Straßburg, H.-J. Lugauer, and A. Hoffmann, "Temperature-dependent recombination coefficients in InGaN light-emitting diodes: hole localization, Auger processes, and the green gap," Appl. Phys. Lett. **109**, 161103 (2016).
27. A. L. Efros and M. E. Raikh, "Effect of composition disorder on the electronic properties of semiconducting mixed crystals," in *Optical Properties of Mixed Crystals*, R. J. Elliott and I. P. Ipatova, eds. (Elsevier, 1988), pp. 135–175.
28. P. R. C. Kent and A. Zunger, "Carrier localization and the origin of luminescence in cubic InGaN alloys," Appl. Phys. Lett. **79**, 1977–1979 (2001).
29. S. Schulz, M. A. Caro, C. Coughlan, and E. P. O'Reilly, "Atomistic analysis of the impact of alloy and well-width fluctuations on the electronic and optical properties of InGaN/GaN quantum wells," Phys. Rev. B **91**, 035439 (2015).
30. M. Auf der Maur, A. Pecchia, G. Penazzi, W. Rodrigues, and A. Di Carlo, "Efficiency drop in green InGaN/GaN light emitting diodes: the role of random alloy fluctuations," Phys. Rev. Lett. **116**, 027401 (2016).
31. S. L. Chuang and C. S. Chang, "k·p method for strained wurtzite semiconductors," Phys. Rev. B **54**, 2491–2504 (1996).
32. K. Kojima, M. Funato, Y. Kawakami, and S. Noda, "Valence band effective mass of non-c-plane nitride heterostructures," J. Appl. Phys. **107**, 123105 (2010).
33. http://www.str-soft.com/products/SiLENSe/index.htm.
34. E. Kioupakis, P. Rinke, K. T. Delaney, and C. G. Van de Walle, "Indirect Auger recombination as a cause of efficiency droop in nitride light-emitting diodes," Appl. Phys. Lett. **98**, 161107 (2011).
35. F. Bertazzi, M. Goano, and E. Bellotti, "Numerical analysis of indirect Auger transitions in InGaN," Appl. Phys. Lett. **101**, 011111 (2012).
36. B. Galler, H.-J. Lugauer, M. Binder, R. Hollweck, Y. Folwill, A. Nirschl, A. Gomez-Iglesias, B. Hahn, J. Wagner, and M. Sabathil, "Experimental determination of the dominant type of Auger recombination in InGaN quantum wells," Appl. Phys. Express **6**, 112101 (2013).
37. F. Bertazzi, X. Zhou, M. Goano, G. Ghione, and E. Bellotti, "Auger recombination in InGaN/GaN quantum wells: a full-Brillouin-zone study," Appl. Phys. Lett. **103**, 081106 (2013).
38. M. J. Davies, P. Dawson, S. Hammersley, T. Zhu, M. J. Kappers, C. J. Humphreys, and R. A. Oliver, "Comparative studies of efficiency droop in polar and non-polar InGaN quantum wells," Appl. Phys. Lett. **108**, 252101 (2016).
39. G. B. Stringfellow, "Microstructures produced during the epitaxial growth of InGaN alloys," J. Cryst. Growth **312**, 735–749 (2010).